Journal of Electrochemistry

Volume 25
Issue 2 *Special Issue: Electrochemical Analysis and Sensing (I)*

2019-04-28

Graphene-Like Secondary-Laser-Etched Polyimide Film Decorated with Cu_xO Nanocomposites: A Novel Electrode Substrate for Non-Enzymatic Glucose Sensors

Wan-lin DAI

Zhi-wei LU

Jian-shan YE
School of Chemistry and Chemical Engineering, South China University of Technology,Guangzhou 510641, P.R. China;, jsye@scut.edu.cn

Recommended Citation
Wan-lin DAI, Zhi-wei LU, Jian-shan YE. Graphene-Like Secondary-Laser-Etched Polyimide Film Decorated with Cu_xO Nanocomposites: A Novel Electrode Substrate for Non-Enzymatic Glucose Sensors[J]. *Journal of Electrochemistry*, 2019 , 25(2): 260-269.
DOI: 10.13208/j.electrochem.181052
Available at: https://jelectrochem.xmu.edu.cn/journal/vol25/iss2/11

DOI: 10.13208/j.electrochem.181052 **Artical ID**:1006-3471(2019)02-0260-10
Cite this: *J. Electrochem.* **2019**, *25*(2): 260-269 **Http**://electrochem.xmu.edu.cn

Graphene-Like Secondary-Laser-Etched Polyimide Film Decorated with Cu_xO Nanocomposites: A Novel Electrode Substrate for Non-Enzymatic Glucose Sensors

DAI Wan-lin, LU Zhi-wei, YE Jian-shan*
(*School of Chemistry and Chemical Engineering, South China University of Technology, Guangzhou* 510641, *P.R. China*)

Abstract: In this work, a novel electrode substrate with graphene-like surface and Cu_xO nanocomposites derived from secondary-laser-etched polyimide (SLEPI) film was synthesized and applied in non-enzymatic glucose detection for the first time. Characterizations indicate that the as-prepared SLEPI/Cu_xO film electrode (SLEPI/Cu_xO-FE) possessed huge surface area, plentiful active sites and excellent electrocatalytic performance. The obtained sensor exhibited the high sensitivity and selectivity for glucose determination with a linear range of 0.05 mmol·L^{-1} to 3 mmol·L^{-1} and a detection limit of 1.72 μmol·L^{-1} (*S*/*N*=3), which provides a simple, flexible and low-cost electrochemical sensor for diabetes diagnosis.

Key words: electrochemical sensor; laser-etched; polyimide; Cu_xO nanocomposite; glucose; non-enzymatic
CLC Number: O646 **Document Code**: A

Diabetes mellitus, characterized by persistent hyperglycemia, is a metabolic disease caused by insufficient insulin secretion or insensitivity of peripheral tissues to insulin. It may cause long term damage, insufficiency or failure of various tissues and organs (such as eyes, kidneys, heart, blood vessels, and nerves)[1]. According to statistics, about 451 million people aged 18 ~ 99 years old in the world suffered from diabetes in 2017 (prevalence rate 8.4%), and another 374 million have impaired glucose intolerance (prevalence rate 7.7%)[2]. China has the largest number of diabetics in the world. In 2015, the number of patients in China reached 109.6 million, and 1.3 million people died of diabetes and its complications[3]. At the same time, according to the prediction from International Diabetes Federation (IDF), if there is no intervention, global diabetes patients will reach 693 million in 2045, presenting a large burden in social, financial and health systems across the world[2].

At present, there is no complete cure for diabetes. Controlling blood glucose is the core of diabetes treatment. Therefore, a rapid and accurate determination of glucose concentration in blood is crucial for diagnosis and monitoring of diabetes[4]. Over the years, many efforts have been paid to develop the fast, sensitive and low-cost analytical methods for glucose testing. Biochemical analyzers are commonly used in clinical blood glucose detection because of high accuracy. However, it takes more blood with more complicated procedure on sample pretreatment, which may need a long time and delay the medical treatment. In contrast, enzyme glucose meters are widely used in rapid and high efficiency determination. But the stability of the enzyme-based tester is restricted to temperature, pH, humidity and other conditions[5]. For all the above factors, researchers pay more and more attentions on non-enzymatic glucose sensors constructed by glucose oxidation catalysts such as noble metals[6], alloys[7] and metal oxides[8]. Specifically, copper nanomaterials have been widely investigated due to their good catalytic activity to glucose oxidation in an alkaline medium[9-12].

Received: 2018-12-18, Revised: 2019-02-22 *Corresponding author, Tel: (86-20)87113241, E-mail: jsye@scut.edu.cn

Graphene and graphene-like materials, which are used as supporting substrates for nanostructure catalysts due to their high conductivity, large surface area and good chemical stability[13]. For instance, various kinds of copper/graphene nanocomposites have been prepared for glucose detection[14-16]. Recently, an electrode employing direct laser-scribed polyimide has becoming as a new type of flexible and disposable electrode which has a graphene-like surface and properties. The one-step synthesis of laser-scribed graphene (LEG) has opened a new wide horizon for applications of electrochemical sensing[17-18]. Our group reported a micro-patterned and miniaturized flexible electrode formed by the laser-scribed polyimide films for electrochemical sensing of heavy metal ions [19]. The laser-scribed polyimide film process to obtain graphene-like nanomaterials possessed hierarchical porous structure, which improves the sensing capacity of the electrode material. Considering the good physical and chemical characteristics of copper and graphene, thus, copper/graphene hybrid materials may possess superior performance. At present, the biggest challenge in manufacturing graphene/metal-based hybrid materials is the lengthy process [20]. Compared with mechanical mixing, the wet-chemistry integration of laser secondary scribing is seemingly straightforward. However, to our best knowledge, secondary-lasered polyimide/Cu_xO film electrode for the electrochemical glucose biosensor has not been reported.

In this work, Laser-scribed polyimide film electrode sensors with graphene-liked surface and decorated with copper oxide nanocomposites (secondary-laser-etched polyimide/Cu_xO film electrode, SLEPI/Cu_xO-FE) were fabricated by a simple laser-adsorption-laser process and applied in non-enzymatic glucose determination (Fig. 1). The first laseretching step would create a graphene-like electrode surface with large specific area and enhance the adsorption of Cu(II) ions, while the second one would partly reduce the adsorbed copper ions to Cu_xO nanocomposites which were evenly distributed on the graphene layers. Owing to the distinct morphology and structure, the nanoparticles-decorated sensor exhibited excellent catalytic activity for glucose oxidation, even though the content of copper was extremely low (0.16at%).

1 Experimental

1.1 Materials and Reagents

Polyimide membrane (125 nm) was purchased from Mei Xin Jue Yuan Material Co., Ltd. Glucose was bought from Aladdin Biochemical Technology Co., Ltd. (Shanghai, China). Ascorbic acid (AA) was obtained from Sinopharm Chemical Reagent Co. Ltd (China), and dopamine (DA) and uric acid (UA) were purchased from Sigma-Aldrich. L-cysteine was obtained from Adamas. Copper sulfate pentahydrate ($CuSO_4 \cdot 5H_2O$) and other reagents were purchased from local distributors, and were of analytical grade and used without further purification. Ultra-pure water (> 18.4 MΩ·cm) was used throughout. The human blood serum samples were obtained from the hospital on campus and the related experiments were performed following the WHO guidelines on blood drawing (WHO Publication ISBN-13: 978-92-4-159922-1, 2010).

1.2 Apparatuses

The morphology and size of the electrode surface were investigated by scanning electron microscope (SEM, Merlin, Zeiss) equipped with an EDX analyzer and transmission electron microscope (TEM, JEM-2100F, JOEL, Japan). X-ray diffraction spectrometer (XRD, D8 ADVANCE, Bruker, Germany) and X-ray photoelectron spectroscope (XPS, ESCALAB 250Xi spectrometer, K-Alpha, Thermo Fisher Scientific, USA) were used to analyze the structure and chemical composition of the electrode material, respectively. Other physical properties were characterized through Raman spectroscope (Aramis LabRam spectrometer, H J Y, Ltd., France).

Cyclic voltammetry (CV), electrochemical impedance spectroscopy (EIS) and amperometric measurements were carried out using an IGS-6030 electrochemical workstation (Guangzhou Ingsens Sensor Technology Co., Ltd, China) with a three-electrode system, consisted of a laser-scribed polyimide film

based working electrode, a platinum wire counter electrode and an Ag/AgCl (3 mol·L^{-1} KCl) reference electrode. Amperometric *i-t* measurement was performed in 0.1 mol·L^{-1} NaOH solution with steady magnetic stirring.

1.3 Preparations of SLEPI/Cu_xO-FE

All laser scribing was finished by a JL-K3020 laser engraving machine (Liaocheng Julong Laser Equipment Co., Ltd, China). The preparations of SLEPI/Cu_xO-FE were done in several simple steps as follows. Firstly, a piece of polyimide substrate was put in the laser engraving machine and etched by laser beam according to the preset pattern, and the first laser etched polyimide film electrode (FLEPI-FE) patterns were achieved (Fig. 1(A)). Secondly, the FLEPI-FE substrate was immersed in 0.5 mol·L^{-1} $CuSO_4$ solution for 24 h to adsorb the Cu(II) cations into the graphene layers (Fig. 1(B)), and then dried in an oven at 70 ℃. Thirdly, the electrode surface of the patterns was laser-scribed once again, leading to the formation of homogenously dispersed copper nanocomposites onto the graphene-like electrode surface (Fig. 1(C)). Then the substrate was washed with ultrapure water to remove the remaining copper salt and dried in N_2 flow. The as-prepared electrode patterns were then cut into single piece of electrodes, noted as SLEPI/Cu_xO-FE. As can be seen in Fig. 1(D), the conducting pathway between the connector and the electrode surface was sealed with paint to insulate the conductive path between the electrode surface and the connecting surface. In the meantime, SLEPI/-FE without immersion in $CuSO_4$ solution were fabricated for control experiments.

2 Results and Discussion

2.1 Characterizations

The fabricated SLEPI/Cu_xO-FE was characterized by SEM, TEM, XRD and XPS. Fig. 2(A) and (B) shows the SEM images of the SLEPI-FE and the SLEPI/Cu_xO-FE. As shown in Fig. 2(A), the porous structure of three-dimensional graphene was formed after the secondary laser scribing process, which is similar to our previous results[18]. Upon incorporating

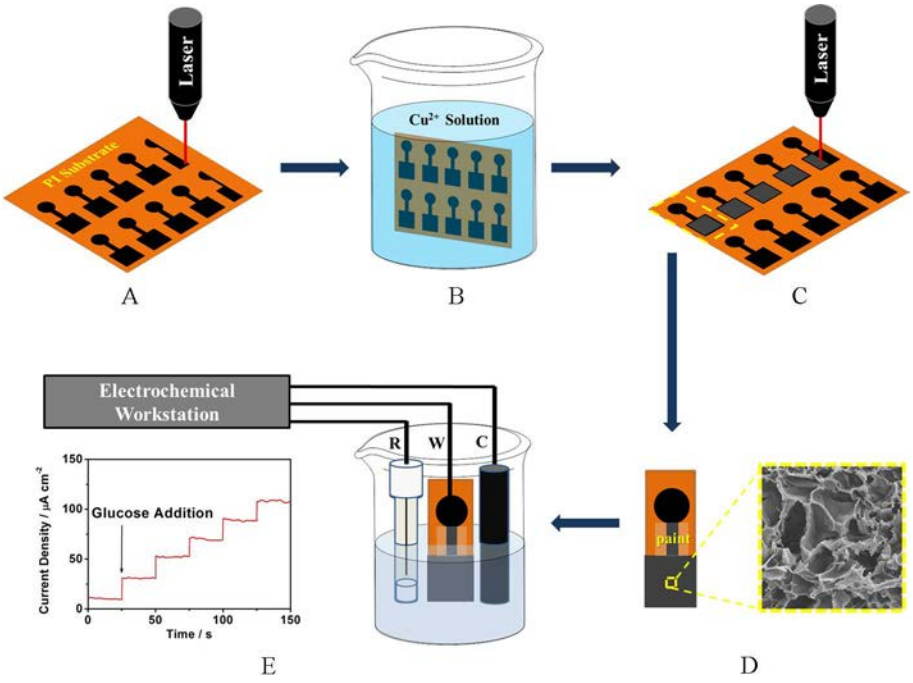

Fig. 1 Schematic illustration for the fabrication of SLEPI/Cu_xO-FE patterns on PI substrate. (A) Fabrication of FLEPI-FE patterns by laser scribing. (B) FLEPI-FE patterns immersed in Cu(II) solution for adsorption of Cu(II) into the graphene layers. (C) Fabrication of SLEPI/Cu_xO-FE patterns by laser scribing on electrode surface. (D) Sketch of a SLEPI/Cu_xO-FE sensor cut from the SLEPI/Cu_xO-FE substrate and SEM image of the electrode surface with homogenously dispersed Cu_xO nanocomposites. (E) Non-enzymatic glucose detection with amperometric method.

copper nanoparticles onto SLEPI-FE substrate, the corresponding SEM image of SLEPI/Cu_xO-FE is shown in Fig. 2(B). The wet-chemistry integration of laser secondary scribing process led to a rough surface. Elemental mapping results indicated the uniform distributions of elemental C, Cu and O in the SLEPI/Cu_xO-FE (Fig. 2(C)).

To further investigate the morphology and composition of the nanocomposites, the surface material of SLEPI/Cu_xO-FE was scraped from the PI substrate and observed by TEM. Fig. 2(D-E) confirmed that the nanoparticles with a diameter up to 50 nm were distributed in the porous and wrinkled graphene layers. The high resolution TEM image in Fig. 2(F) verified the existences of graphene layers and copper nanoparticles. Moreover, the elemental mapping results in a magnified view in Fig. 2(G) corroborates that the nanoparticles were mainly composed of copper.

The XPS spectra in Fig. 3(A)-(B) and XRD patterns in Fig. 3(C) further depict the composition of the SLEPI-PE with the SLEPI/Cu_xO-FE. It is estimated that the electrode surface had a basis containing 97.93at% of carbon, 0.61at% of nitrogen and 1.31at% of oxygen which mainly derived from the PI substrate, and 0.16at% of Cu adsorbed from the Cu(II) solution and partly reduced by the laser etching process. The

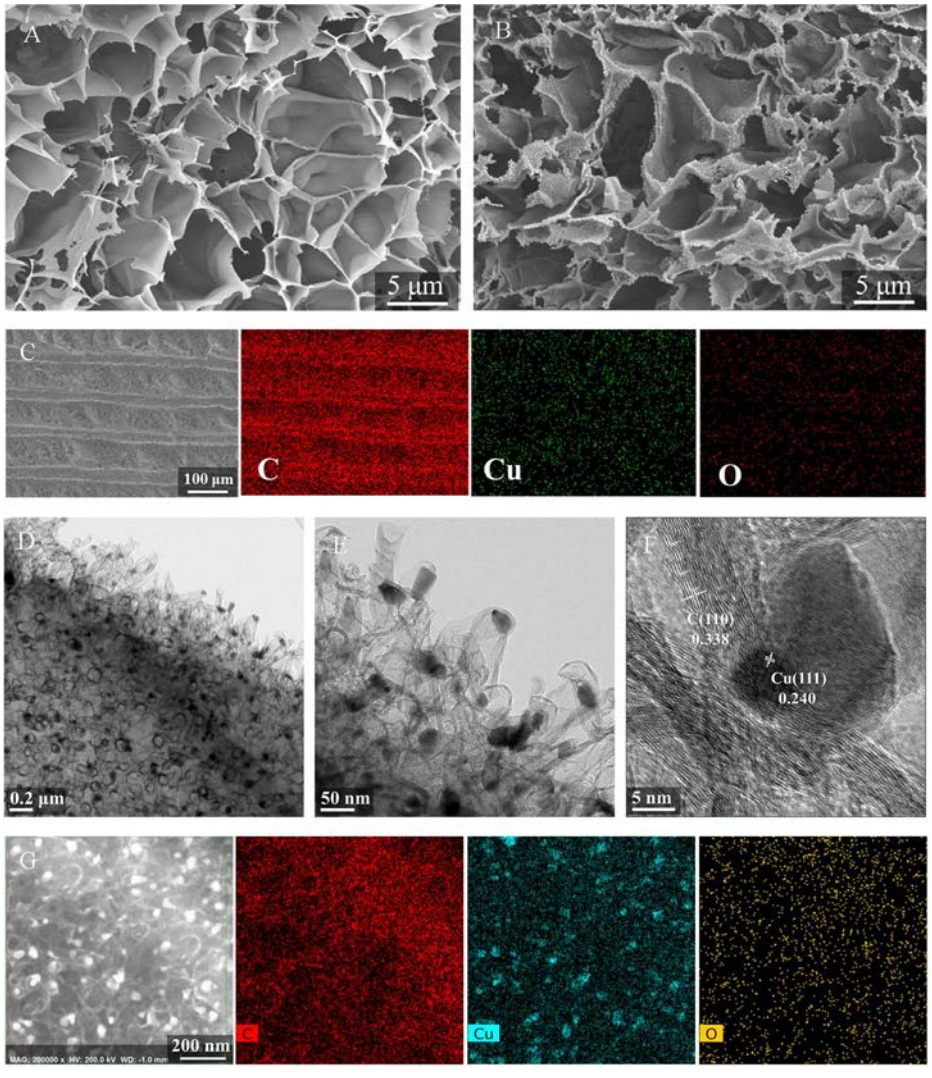

Fig. 2 SEM images of SLEPI-FE (A), SLEPI/Cu_xO-FE (B) and the corresponding elemental mapping images of C, Cu, O elements in SLEPI/Cu_xO-FE (C); TEM images of SLEPI/Cu_xO-FE at different resolutions (D-F) and the corresponding elemental mapping images of C, Cu, O elements in SLEPI/Cu_xO-FE (G).

high resolution Cu 2p spectrum in Fig. 3(B) reveals the presences of several peaks at 932.2, 934.0, 941.8, 952.1 and 954.0 eV. The peaks at 932.2 eV and 952.1 eV were most likely due to Cu $2p_{3/2}$ and Cu $2p_{1/2}$, which are from Cu(0) or Cu_2O[15]. The broadened peak at 941.8 eV suggested the presence of Cu(II). The overlapping peaks of Cu $2p_{3/2}$ (932.2, 934.0 eV) and Cu $2p_{1/2}$ (952.1, 954.0 eV) revealed the co-existence of Cu(0), Cu(I) and Cu(II)[15, 21], which means that the secondary-laser-etched process partly reduced the adsorbed copper salt to Cu(0) and Cu(I) in ambient air. In Fig. 3(C), the SLEPI/Cu_xO-FE showed obvious peaks at 43.30°, 50.43° and 74.13° indexed to the (111), (200), (220) planes of copper (JCPDS No. 04-0836), respectively, indicating a higher content of Cu(0) in the nanoparticles, and the responses of other co-existing forms might be covered up. Besides, the curve b in Fig. 3(C) proved that no obvious change in the composition of SLEPI/Cu_xO-FE occurred after the amperometric detection. Based on the multi-valence property and huge specific surface area, the SLEPI/Cu_xO-FE sensor may offer abundant active sites for the electrocatalysis of glucose.

Furthermore, the Raman spectra of the FLEPI-FE, SLEPI-FE and SLEPI/Cu_xO-FE were investigated and the results are shown in Fig. 3(D). It is evident that all the electrode samples revealed the presences of three prominent features at 1356 cm^{-1} for D band, 1585 cm^{-1} for G band and 2700 cm^{-1} for 2D band. The intensity ratio of the D and G bands (I_D/I_G) is used to evaluate the degrees of graphitic carbon[22]. The I_D/I_G values were observed in a decreasing order as follows: SLEPI-FE (0.602) > FLEPI-FE (0.562) > SLEPI/Cu_x-O-FE (0.232), indicating a gradual increase in crystallinity after the incorporation of Cu_xO nanoparticles. Besides, the appearances of obvious 2D band further

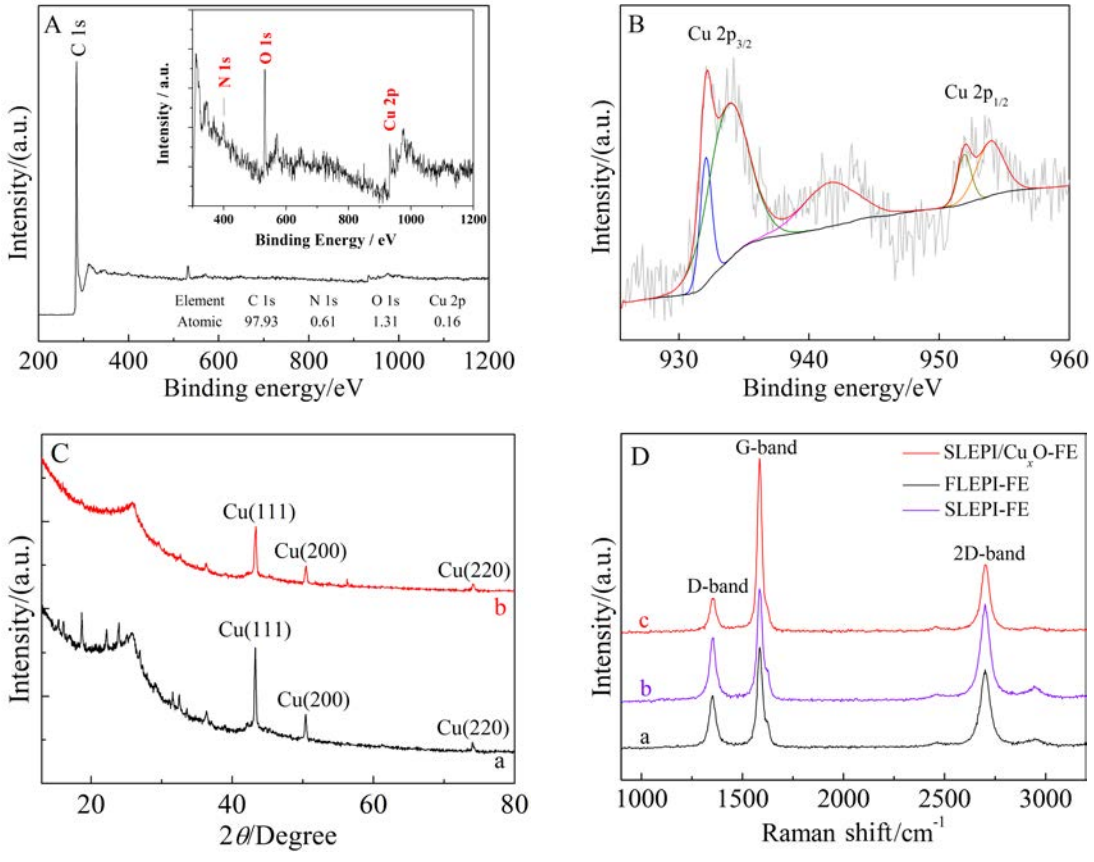

Fig. 3 (A) XPS survey spectrum (the inset shows the enlarged spectrum for N 1s, O 1s and Cu 2p) and (B) high resolution Cu 2p spectrum of SLEPI/Cu_xO-FE; (C) XRD patterns of SLEPI/Cu_xO-FE before (a) and after (b) the amperometric detections; (D) Raman spectra of FLEPI-FE (a), SLEPI-PE (b) and SLEPI/Cu_xO-PE (c).

indicated the presence of 3D multilayer graphene structure, which is in good agreement with the SEM results.

2.2 Electrochemical Behaviors

Fig. 4(A) displays the cyclic voltammograms (CVs) of SLPI-FE and SLEPI/Cu_xO-FE in the absence and presence of 0.1 mol·L^{-1} glucose in 0.1 mol·L^{-1} NaOH solution at a scan rate of 100 mV·s^{-1}. As shown in Fig. 4(A), there was no distinct redox peak at the CV of SLEPI-FE (Curve b) when 0.2 mmol·L^{-1} of glucose was added into the solution. By contrast, an oxidation peak at the potential of 0.5 V approximately was clearly observed in CV of SLEPI/Cu_xO-FE with addition of glucose (Curve d), demonstrating that the SLEPI/Cu_xO-FE has electrocatalytic activity for the electro-oxidation of glucose, which may be attributed to the introduction of copper nanoparticles from the second laser etched process.

Meanwhile, EIS was used to investigate the interfacial electron transfer resistance (R_{et}). Fig. 4(B) displays the Nyquist plots of electrochemical impedance spectra of different electrodes in 5.0 mmol·L^{-1} $K_3Fe(CN)_6/K_4Fe(CN)_6$ (1:1) containing 0.1 mol·L^{-1} KCl with a frequency range of 0.01 Hz ~ 100 kHz under open circuit potential. As shown in Fig. 4(B), comparing with a relatively large R_{et} on SLPI-FE (b), smaller semicircle on SLEPI/Cu_xO-FE (a) was obtained. Significantly reduced R_{et} was attributed to the fact that the enlarged specific area and high electrical conductivity, which improved the electron transfer and mass exchange of electroactive indicators on the film surface[23]. Thus, these results show that the as-prepared SLEPI/Cu_xO-FE is better in conductivity due to the existence of copper nanoparticles.

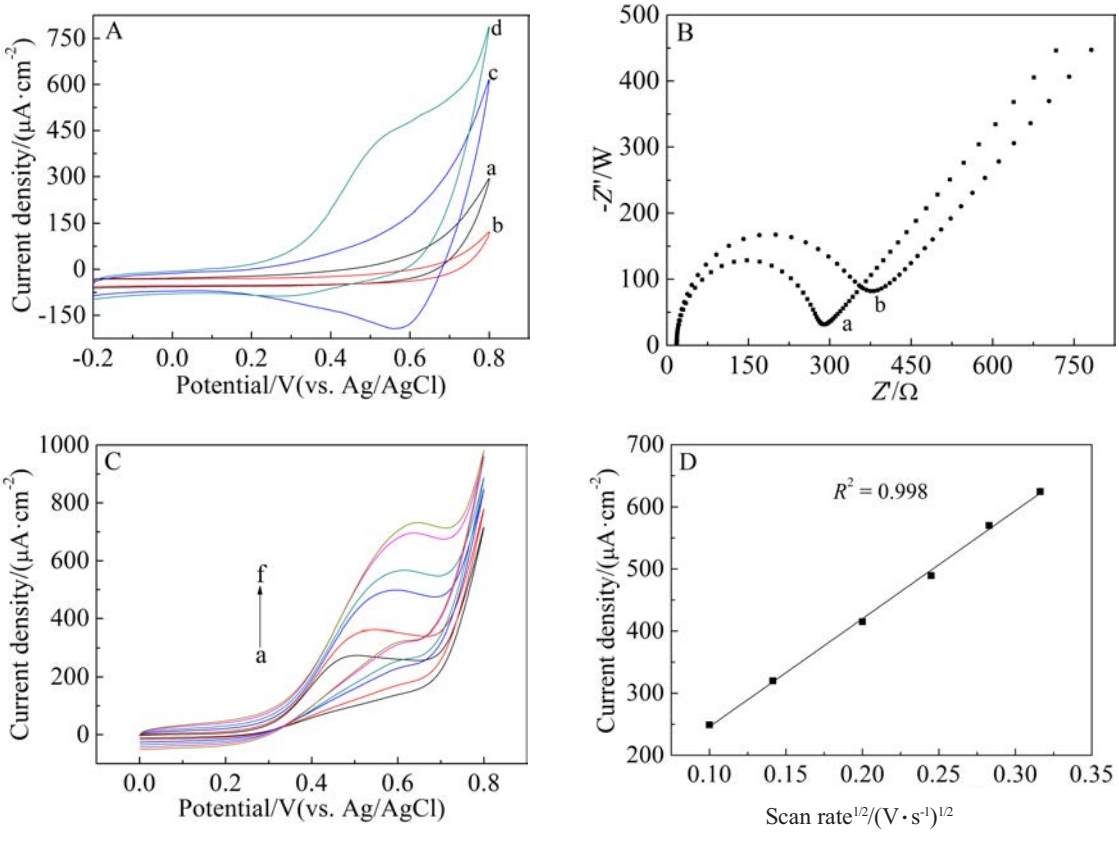

Fig. 4 (A) CVs of SLEPI-FE (a, b) and SLEPI/Cu_xO-FE (c, d) in the absence (a, c) and presence (b, d) of 0.2 mmol·L^{-1} glucose in 0.1 mol·L^{-1} NaOH. Scan rate: 100 mV·s^{-1}. (B) Electrochemical impedance spectra for the SLEPI-FE (a) and SLEPI/Cu_xO-FE (b) in 5.0 mmol·L^{-1} $K_3Fe(CN)_6/K_4Fe(CN)_6$ (1:1) containing 0.1 mol·L^{-1} KCl. (C) CVs of the SLEPI/Cu_xO-FE in 0.1 mol·L^{-1} NaOH containing 0.5 mmol·L^{-1} glucose at different scan rates, a to f: 0.01, 0.02, 0.04, 0.06, 0.08, 0.1 V·s^{-1}. (D) Anodic peak current density as a function of square root of scan rate with a linear fitting.

CVs of the SLEPI/Cu_xO-FE in 0.1 mol·L^{-1} NaOH containing 0.5 mmol·L^{-1} glucose at different scan rates (from 0.01 to 0.1 V·s^{-1}) were recorded and are presented in Fig. 4(C). As shown in Fig. 4(C), when the scan rate increased, the oxidation peak current density of glucose was increased and the peak potential was shifted towards the positive direction slightly. A linear relationship between the anodic peak current density and the square root of scan rate was observed in Fig. 4(D), and the linear regression equation is $I_p(\mu A \cdot cm^{-2}) = 1739.06v^{1/2}(V^{1/2} \cdot s^{-1/2}) + 72.19$ with a correlation coefficient of 0.998, indicating that the oxidation of glucose at SLEPI/Cu_xO-FE was a diffusion-controlled process[24].

Above explorations showed that the SLEPI/Cu_xO-FE effectively integrated the excellent properties of laser etched graphene and Cu_xO, and exhibited several attractive features with a significantly large active area, an excellent electrical conductivity, and an enhanced catalytically active site. All of these advantages make it a promising candidate for high performance electrochemical applications.

2.3 Amperometric Detection of Glucose

The amperometric responses on the SLEPI/Cu_xO-FE after the subsequent addition of glucose in 0.1 mol·L^{-1} NaOH at an applied potential of 0.6 V are shown in Fig. 5. The corresponding calibration curve with linear regression is inserted in Fig. 5. Upon successive addition of glucose with homogeneous stirring, the current response increased rapidly, indicating that the SLEPI/Cu_xO-FE sensor electrode exhibited an excellent electrocatalytic activity. As shown in Fig. 5, the SLEPI/Cu_xO-FE sensor displays a linear

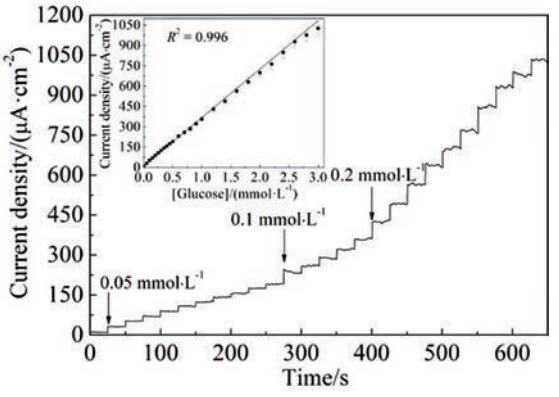

Fig. 5 Real-time amperometric response of the SLEPI/Cu_xO-FE to the successive addition of glucose in 0.1 mol·L^{-1} NaOH at an applied potential of 0.6 V. Insert: the corresponding calibration curve with linear fitting.

range from 0.05 mmol·L^{-1} to 3.0 mmol·L^{-1} and a detection limit of 1.72 μmol·L^{-1} (S/N=3). The corresponding regression equation is $I(\mu A \cdot cm^{-2}) = 10.51 + 357.63[\text{Glucose}](\text{mmol} \cdot L^{-1})$, R^2=0.996. Compared with some previous reports for the determination of glucose in 0.1 mol·L^{-1} NaOH electrolyte in Table 1, it can be seen that SLEPI/Cu_xO-FE had the characteristics of high sensitivity, low detection limit and fast response time, ascribed to the electrocatalytic active region and promoted electron transfer during the oxidation of glucose.

2.4 Interference, Reproducibility, Long-Term Stability and Real Sample Analysis

The anti-interference property of the non-enzymatic sensor is essential to the determination of glucose. Some oxidizable molecules, such as ascorbic acid (AA), dopamine (DA), uric acid (UA), L-cysteine, and other carbohydrates, may coexist with glucose in

Tab. 1 Comparison of non-enzymatic electrochemical glucose sensors in 0.1 mol·L^{-1} NaOH solution

Electrode material	Sensitivity/ ($\mu A \cdot (mmol \cdot L^{-1})^{-1} \cdot cm^{-2}$)	Linear range/ (mmol·L^{-1})	Detection limit/ (μmol·L^{-1})	Working potential/V	Ref.
Cu_3N NA/CF	14180	0.001~2.0	0.013	0.40 (vs. Hg/HgO)	[25]
Co_3N NW/TM	139.9	0.002~28	1	0.60 (vs. Hg/HgO)	[26]
Ni_2P NA/CC	7792	0.001~3.0	0.18	0.50 (vs. SCE)	[27]
CuO/Nafion/GCE	1783.58	0.01~0.30	0.80	0.60 (vs. Ag/AgCl)	[28]
SLEPI/Cu_xO-FE	368.14	0.05~3.0	1.72	0.60 (vs. Ag/AgCl)	This work

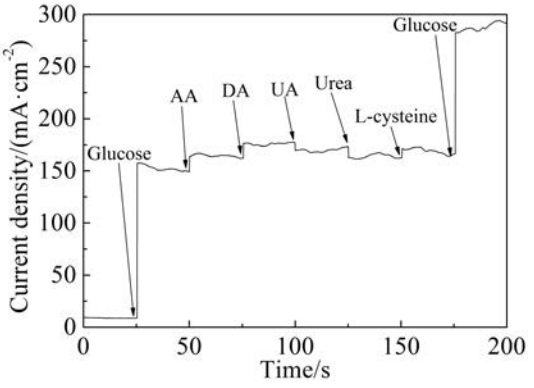

Fig. 6 Glucose selectivity study with various interferences compounds. Amperometric response of the electrode to 0.5 mmol·L^{-1} glucose, 0.05 mmol·L^{-1} AA, 0.05 mmol·L^{-1} DA, 0.05 mmol·L^{-1} UA, 0.05 mmol·L^{-1} Urea, 0.05 mmol·L^{-1} L-cysteine and 0.5 mmol·L^{-1} glucose at an applied voltage of 0.6 V (vs. Ag/AgCl), respectively.

some actual samples and interfere with the glucose detection. Considering the concentrations of glucose and interfering species in blood samples, for instance, 0.5 mmol·L^{-1} glucose, 0.05 mmol·L^{-1} AA, 0.05 mmol·L^{-1} DA, 0.05 mmol·L^{-1} UA, 0.05 mmol·L^{-1} urea, 0.05 mmol·L^{-1} L-cysteine and 0.5 mmol·L^{-1} glucose were subsequently added into 0.1 mol·L^{-1} NaOH at an applied potential of 0.6 V (vs. Ag/AgCl) by amperometric measurement. According to the amperometric response shown in Fig. 6, the fabricated sensor had good selectivity and anti-interference property for the oxidation of glucose comparing with other coexisting species in the solution.

The reproducibility of the SLEPI/Cu_xO-FE sensor was evaluated by measuring the current responses to 10 successive additions of 0.05 mmol·L^{-1} glucose into 0.1 mol·L^{-1} NaOH at 5 different electrodes prepared under the same conditions, and the relative standard deviation (RSD) was 5.6%, indicating the good reliability and good reproducibility of the sensor. The long-term stability of the sensor was measured by testing the current response of the sensor after one-month storage at 4 °C, and the result was 10.2% lower compared to its initial state, which reveals the good stability of SLEPI/Cu_xO-FE.

Finally, the SLEPI/Cu_xO-FE sensor was applied to the determination of glucose in human blood serum. 50 μL of human blood serum sample was mixed with 5 mL 0.1 mol·L^{-1} NaOH solution and the current response was measured at 0.6 V. Afterwards, standard solution of glucose was injected subsequently at 25 s intervals for three times. The results calculated from the calibration curve in Fig. 5 are tabulated in Table 2. Nevertheless, we found that the SLEPI/Cu_xO-FE sensor was non-reusable as the amperometric response decreased distinctly in a second test, which may be due to the electrode surface pollutions of proteins and other substances. In consideration of inexpressive, sensitive and non-reusable properties, the SLEPI/Cu_xO-FE could be used as disposable sensors in real sample analysis.

3 Conclusions

In summary, we developed a non-enzymatic glucose sensor based on a flexible and disposable secondary-laser-etched polyimide film electrode with graphene-like porous surface and decorated with Cu_xO nanocomposites. The sensor had advantageous properties such as high surface area, high conductivity and excellent electrocatalytic activity towards glucose oxidation in an alkaline medium. The newly de-

Tab. 2 Comparison of glucose detection in human serum samples by the SLEPI/Cu_xO-FE sensor and the biochemical analyzer from hospital

Sample	Glucose sensor in this work/ (mmol·L^{-1})	Results from hospital/ (mmol·L^{-1})	Recovery%
1	8.44	8.13	103.8
2	7.27	7.23	100.6
3	6.32	6.47	97.7

veloped non-en zymatic glucose sensor presented a number of attractive analytical features such as long-term stability, reproducibility and selectivity. The electrochemical measurements proved that the SLEPI/Cu_xO-FE has a great potential in non-enzymatic glucose determination.

Acknowledgements

This work was supported by Science and Technology Program of Guangdong Province (No. 2019B020219002, No. 2018A050506006), Natural Science Foundation of Guangdong Province (No. 2017A030312005) and National Natural Science Foundation of China (NSFC, No. 21875070).

References:

[1] Wang J. Electrochemical glucose biosensors[J]. Chemical Reviews, 2008, 108(2): 814-825.

[2] Cho N H, Shaw J E, Karuranga S, et al. IDF Diabetes Atlas: Global estimates of diabetes prevalence for 2017 and projections for 204[J]. Diabetes Research and Clinical Practice, 2018, 138: 271-281.

[3] Hu C, Jia W P. Diabetes in china: Epidemiology and genetic risk factors and their clinical utility in personalized medication[J]. Diabetes, 2018, 67(1): 3-11.

[4] Han M, Liu S L, Bao J C, et al. Pd nanoparticle assemblies—As the substitute of HRP, in their biosensing applications for H_2O_2 and glucose[J]. Biosensors and Bioelectronics, 2012, 31(1): 151-156.

[5] Hoa L T, Chung J S, Hur S H. A highly sensitive enzyme-free glucose sensor based on Co_3O_4 nanoflowers and 3D graphene oxide hydrogel fabricated via hydrothermal synthesis[J]. Sensors and Actuators B: Chemical, 2016, 223: 76-82.

[6] Chen C, Ran R, Yang Z Y, et al. An efficient flexible electrochemical glucose sensor based on carbon nanotubes/carbonized silk fabrics decorated with pt microspheres[J]. Sensors and Actuators B: Chemical, 2018, 256: 63-70.

[7] Wang J P, Gao H, Sun F L, et al. Nanoporous PtAu alloy as an electrochemical sensor for glucose and hydrogen peroxide[J]. Sensors and Actuators B: Chemical, 2014, 191: 612-618.

[8] Marimuthu T, Mohamad S, Alias Y. Needle-like polypyrrole-NiO composite for non-enzymatic detection of glucose[J]. Synthetic Metals, 2015, 207: 35-41.

[9] Zhou S H, Feng X, Shi H Y, et al. Direct growth of vertically aligned arrays of $Cu(OH)_2$ nanotubes for the electrochemical sensing of glucose[J]. Sensors and Actuators B-Chemical, 2013, 177: 445-452.

[10] Cao H M, Yang A L, Li H, et al. A non-enzymatic glucose sensing based on hollow cuprous oxide nanospheres in a nafion matrix[J]. Sensors and Actuators B: Chemical, 2015, 214: 169-173.

[11] Zhang Y C, Liu Y X, Su L, et al. CuO nanowires based sensitive and selective non-enzymatic glucose detection [J]. Sensors and Actuators B: Chemical, 2014, 191: 86-93.

[12] Ni P J, Sun Y J, Shi Y, et al. Facile fabrication of CuO nanowire modified Cu electrode for non-enzymatic glucose detection with enhanced sensitivity[J]. RSC Advances, 2014, 4(55): 28842-28847.

[13] Tian J Q, Li H Y, Xing Z C, et al. One-pot green hydrothermal synthesis of CuO-Cu_2O-Cu nanorod-decorated reduced graphene oxide composites and their application in photocurrent generation[J]. Catalysis Science & Technology, 2012, 2(11): 2227-2230.

[14] Hsu Y W, Hsu T K, Sun C L, et al. Synthesis of CuO/graphene nanocomposites for nonenzymatic electrochemical glucose biosensor applications[J]. Electrochimica Acta, 2012, 82(21): 152-157.

[15] Wang Q, Wang Q, Li M, et al. Preparation of reduced graphene oxide/Cu nanoparticle composites through electrophoretic deposition: Application for nonenzymatic glucose sensing[J]. RSC Advances, 2015, 5(21): 15861-15869.

[16] Nia P M, Meng, W P, Lorestani F, et al. Electrodeposition of copper oxide/polypyrrole/reduced graphene oxide as a nonenzymatic glucose biosensor[J]. Sensors and Actuators B: Chemical, 2015, 209: 100-108.

[17] Lin X N, Lu Z W, Zhang Y, et al. A glassy carbon electrode modified with a bismuth film and laser etched graphene for simultaneous voltammetric sensing of Cd(II) and Pb(II)[J]. Microchimica Acta, 2018, 185(9): DOI: 10.1007/s00604-018-2966-4.

[18] Lin X N, Lu Z W, Dai W L, et al. Laser engraved nitrogen-doped graphene sensor for the simultaneous determination of Cd(II) and Pb(II)[J]. Journal of Electroanalytical Chemistry, 2018, 828: 41-49.

[19] Lu Z W, Lin X N, Zhang J J, et al. Ionic liquid/poly-l-cysteine composite deposited on flexible and hierarchical porous laser-engraved graphene electrode for high-performance electrochemical analysis of lead ion[J]. Electrochimica Acta, 2019, 295: 514-523.

[20] Ye R Q, Peng Z W, Wang T, et al. *In situ* formation of metal oxide nanocrystals embedded in laser-induced graphene[J]. ACS Nano, 2015, 9(9): 9244-9251.

[21] Li Z Z, Chen Y, Xin Y M, et al. Sensitive electrochemical nonenzymatic glucose sensing based on anodized CuO nanowires on three-dimensional porous copper foam[J]. Scientific Reports, 2015, 5: 16115.

[22] Veerakumar P, Veeramani V, Chen S M, et al. Palladium nanoparticle incorporated porous activated carbon: Electrochemical detection of toxic metal ions [J]. ACS Applied Materials & Interfaces, 2016, 8(2): 1319-1326.

[23] Wang G F, Wei Y, Zhang W, et al. Enzyme-free amperometric sensing of glucose using Cu-CuO nanowire composites [J]. Microchimica Acta, 2010, 168(1): 87-92.

[24] Yang J, Cho M, Lee Y K. Synthesis of hierarchical $Ni(OH)_2$ hollow nanorod via chemical bath deposition and its glucose sensing performance[J]. Sensors and Actuators B: Chemical, 2016, 222: 674-681.

[25] Wang Z, Cao X Q, Liu D N, et al. Copper-nitride nanowires array: An efficient dual-functional catalyst electrode for sensitive and selective non-enzymatic glucose and hydrogen peroxide sensing[J]. Chemistry - A European Journal, 2017, 23(21): 4986-4989.

[26] Xie F Y, Cao X Q, Qu F L, et al. Cobalt nitride nanowire array as an efficient electrochemical sensor for glucose and H_2O_2 detection[J]. Sensors and Actuators B: Chemical, 2018, 255: 1254-1261.

[27] Chen T, Liu D N, Lu W B, et al. Three-dimensional Ni 2p nanoarray: An efficient catalyst electrode for sensitive and selective nonenzymatic glucose sensing with high specificity[J]. Analytical Chemistry, 2016, 88(16): 7885-7889.

[28] Li Y C(李艳彩), Huang F Y(黄富英), Li S X(李顺兴), et al. Glucose sensor based on the CuO nanoplatelets[J]. Journal of Electrochemistry(电化学), 2014, 20(1): 80-84.

二次刻蚀聚酰亚胺负载 Cu_xO 纳米复合物薄膜电极用于葡萄糖的快速测定

戴琬琳,鲁志伟,叶建山*

(华南理工大学化学与化工学院,广东 广州 510641)

摘要: 本文采用激光刻蚀聚酰亚胺薄膜为载体,浸泡吸附铜离子后经过二次刻蚀还原得到含有 Cu(0)、Cu(I)和 Cu(II)的纳米复合物薄膜电极(SLEPI/Cu_xO-FE). 通过表征可知,SLEPI/Cu_xO-FE 具有大比表面积、丰富的活性位点以及良好的电催化性能. 实验结果表明,该电极对葡萄糖具有良好的电化学响应,并具有较好的稳定性和重现性,有望应用于葡萄糖的低成本检测.

关键词: 电化学传感器;激光刻蚀;聚酰亚胺;Cu_xO 复合材料;葡萄糖;非酶法